

Short Communication

Synthesis and Evaluation of Bamboo-Based Activated Carbon as an Electrode Material for Electric Double Layer Capacitor

Tao Zheng¹, Haixia Zhao², Kouji Nishimoto¹, Tomoya Konishi¹, Masaru Kamano¹, Yoshihiro Okumoto¹, Norikazu Nishiyama³, Tian Xie^{2*}

¹ National Institute of Technology Anan College, 265 Aoki Minobayashi, Anan, Tokushima 774-0017, Japan

² College of Electromechanical Engineering, Qingdao University of Science and Technology, No. 99 Songling Road, Qingdao 266061, China

³ Division of Chemical Engineering, Graduate School of Engineering Science Osaka University, 1-3 Machikaneyama, Toyonaka, Osaka, 560-8531, Japan

*E-mail: qdxt1990@163.com

Received: 27 July 2022 / Accepted: 6 September 2022 / Published: 10 October 2022

Activated carbon (AC_{Mn}) with unique micro-, meso-, and macro-structures has been successfully synthesized using bamboo powder by KMnO₄ activation and pyrolysis carbonization through a one-step strategy. The characteristics and electrochemical performance of the carbon as electrode material for supercapacitors were studied by SEM, TEM, EDX, XRD, N₂ adsorption-desorption, FTIR and CV measurement. The results showed that the AC_{Mn} possesses a porous structure with an efficient specific surface area of 915 m²/g and plenty of micropores. Electrochemical measurements revealed that AC_{Mn} electrode exhibited a high specific capacitance of 225 F/g at the potential scan rates of 2 mV/s. With the increase of potential scan rate, the specific capacitance of based AC_{Mn} based electrode tends to decrease. Compared with AC_k (activated by KOH) based electrode, the decreasing tendency of AC_{Mn}-based electrode is clearly slower. The supercapacitor performance observed is owing to the unique combination of pore structure, it improved both storage capacity and transport behavior. In addition, the electrode has high performance which can be proved by a great variety of surface functional groups, that can improve its electrical conductivity and wettability.

Keywords: activated carbon, bamboo, KMnO₄ activation, pyrolysis carbonization, porous structure

1. INTRODUCTION

Recently, highly efficient, low-cost, green and sustainable energy storage device is urgently required, as the big issues of energy crisis and environmental pollution. In these systems, supercapacitor is attracting attention. Compared with traditional capacitor, supercapacitor has larger specific

capacitance and lithium-ion battery, higher power density and longer service life. Supercapacitor has an absolute advantage in the field of energy storage devices in the future, and it is widely used in military, hybrid vehicles, and intelligent instruments. Carbon material has been considered as one of the most popular electrode materials, which benefit from its, high maximum power density, open porosity, chemical stability environmental friendliness, and low cost [1-3]. Some recent research have presented that carbon nanotube, graphene, and templated carbon has high energy density and specific capacitance [4-6]. However, the scarce raw materials and complicated synthesis processes result in the high cost of carbon materials, which greatly limits the possibility of large-scale production. Thus, it is necessary to explore low-cost carbon material from plenty of renewable resources as electrode materials of supercapacitors.

Currently, renewable biomass material, especially bamboo, has attracted extensive attention as supercapacitor electrode materials [7-9]. Bamboo is a kind of plant with wide range of growth and multi-function. It grows very fast, matures in a short period and has a high production yield. It becomes a serious issue in Japan that bamboo forests gradually enter and expand into mixed forests and plantations, therefore, it is necessary to develop an effective approach for the utilization in particular for high value-added applications of bamboo material [10]. The preparation of biochar with interconnected, multi-channel and porous structure by bamboo carbonization is not only conducive to the penetration of electrolyte and the migration of ions, but also can provide a large accessible surface area, so as to improve the energy storage capacity [9-14]. Therefore, bamboo charcoal can be used as an electrode material for many kinds of electrochemical applications. As a consequently, activated carbon prepared by bamboo can be used as electrode materials not only in electrochemical applications, but also supercapacitor and fuel cell applications. Recently, researchers investigated the feasibility of synthesized activated carbon using bamboo by physical and chemical activation. Compared with physical activation, chemical agent can be impregnated and inlaid into internal structure of precursor during chemical activation. Moreover, AC with well-developed porosity can be obtained through a series of crosslinking and polymerization reaction. Alkali chemical reagents, such as KOH and NaOH, are widely used as chemical activating agents due to their suppression of tar production, which improves the yield of AC. In KOH activation process, the formation of a considerable amount of K_2CO_3 owing to the reaction between KOH and carbon which benefit for the formation of pore structure [15]. The other side of shield, many achievements have been made in using Fe, Co, Ni, Mn and other catalysts to improve the graphitization degree of carbon materials. Thus, the synthesis method of porous biochar mainly adopts the following steps: (1) preparing the bamboo char by carbonized the bamboo powder, (2) an activation step of the bamboo char by activating agents, (3) a graphitization and carbonization step of the bamboo char by graphitization catalyst. However, multi-step processes are time consuming and high cost [16].

In this work, activated carbon (AC_{Mn}) for supercapacitor electrode materials was developed from bamboo powder using potassium permanganate ($KMnO_4$) as the activation agent by one-step strategy. The as-prepared AC_{Mn} and AC_K activated by KOH possess nanoporous structures with a wide specific surface area of $915\text{ m}^2/\text{g}$ and $930\text{ m}^2/\text{g}$, respectively. Additionally, the AC_{Mn} sample has abundant mesopores and macropores. The AC_{Mn} electrode shows a specific capacitance of 73.8 F/g at a potential scan rate of 50 mV/s . Compare with the AC_K electrode (31.1 F/g) it shows higher performance. Furthermore, the results show that in the case of the potential scan rate increased, the capacitance of both

AC_{Mn} and AC_K electrodes will decrease. However, the decreasing rate by AC_K is higher than that of AC_{Mn} . The reason can be considered that the $KMnO_4$ activation process of the bamboo powder makes the meso-macro structure increased, At the same time it also improved the storage capacity and the transport behavior. As a conclusion, the one-step strategy of bamboo powder activated by $KMnO_4$ is considered to be a reasonable method to realize the production for many kinds of energy storage applications with high efficient, low-cost, and sustainable biomass derived carbon materials.

2. EXPERIMENTAL

2.1 Synthesis of porous $KMnO_4$ or KOH activated bamboo-derived carbon

In this work natural bamboo powder which was donated by Bamboo Chemical Laboratory (Tokushima, Japan) is used. To remove the impurities in the bamboo powder it was washed repeatedly with deionized and was dried overnight at 90 °C. Then, the bamboo powder was thoroughly mixed in a $KMnO_4$ solution (1 mol/L) with continuous stirring for 8 hours. After that, it was heated in an oven overnight at 90 °C to obtain a solid mixture. The ratio of bamboo/ $KMnO_4$ is 1:4 by weight. Then, move the prepared mixture into a tube furnace and heated at 800 °C for 2 hours at a heating rate of 5 °C /min in a nitrogen atmosphere. After the temperature of the tube furnace cooled down to the room temperature in nitrogen condition, the activated carbon sample was successfully synthesized. In order to remove the residual inorganic impurities, the prepared samples were cleaned repeatedly by 6 wt% HCl and deionized water. After drying at 90 °C overnight the resultant sample was generated which is denoted as AC_{Mn} .

Another bamboo powder sample which was also dispersed in aqueous KOH solution (1 mol/L, bamboo/ KOH =1:2 by weight) and carbonized under the same conditions is compared for comparison. The resultant sample was denoted as AC_K .

2.2 Physical characterization

Firstly, the morphology of the material was observed using a scanning electron microscope (SEM, JCM-6000, JEOL) and transmission electron microscopy (TEM, H-3000, Hitachi Ltd.). Energy-dispersive X-ray spectroscopy (FE-SEM; SU8010, Hitachi High-Tech America, Inc.) measurement was employed for sample composition analysis. The Fourier transform infrared spectra (FTIR) measurements were carried out using a FT/IR-4200 (JASCO).

The structure of the sample is analyzed by performing X-ray diffraction (XRD, X' Pert PRO MRD, Malvern Panalytical) with Cu $K\alpha$ radiation. The surface characteristics was observed by automated adsorption apparatus (AUTOSORB-1, Quantachrome Co.). In the experiment, nitrogen gas physisorption is used at 77 K. In the end, using the Brunauer- Emmett-Teller (BET) and the Barrett-Joyner-Halenda (BJH) equation, the specific surface area and pore size distribution of the sample was evaluated.

2.3 Electrochemical measurement

Electrochemical performance of a single AC_{Mn} and AC_K electrodes were measured by a three-electrode system. First of all, electrodes based on AC_{Mn} and AC_K were fabricated. The mixed sample includes 70 wt% sample powders, 20 wt% carbon black (as the electrical conductor) and 10 wt% polytetrafluorethylene (as the binder). The sample was milled to produce a homogeneous sheet. After that, the sheet was cut to a smaller sheet of $1 \times 1 \text{ cm}^2$ as the electrodes sheet. The densities of the electrode sheets were about 20 mg/cm^2 for all electrodes.

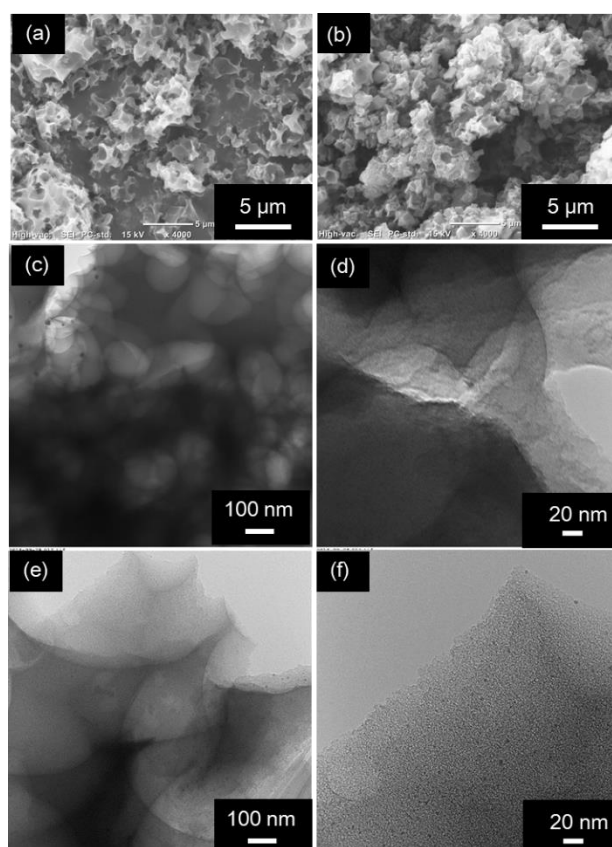


Figure 1. SEM images of AC_{Mn} (a) and AC_K (b) samples; TEM images of AC_{Mn} (c, d) and AC_K (e, f).

The electrochemical performance of the single electrode based on AC_{Mn} and AC_K was investigated by three-electrode system (using a Pt mesh current-collector). The platinum plate and silver–silver chloride ($Ag/AgCl$) electrode was used as the counter electrode and reference electrode, respectively. The three electrodes were immersed into 1 M H_2SO_4 electrolyte solutions and degassed under vacuum for 2 hours prior to the electrochemical testing. Cyclic voltammetry (CV) measurements were performed at a potential scan rate ranging from 2 to 100 mV/s. The specific capacitance (C , F/g) was calculated from CV profiles according to the equation $C = \Delta I / 2mv$, where ΔI is the current difference between charge and discharge when the voltage is 0.4 V, m is the mass of active materials, v is the scan rates of voltage [17].

3. RESULTS AND DISCUSSION

3.1 Characterization of AC_{Mn} and AC_K

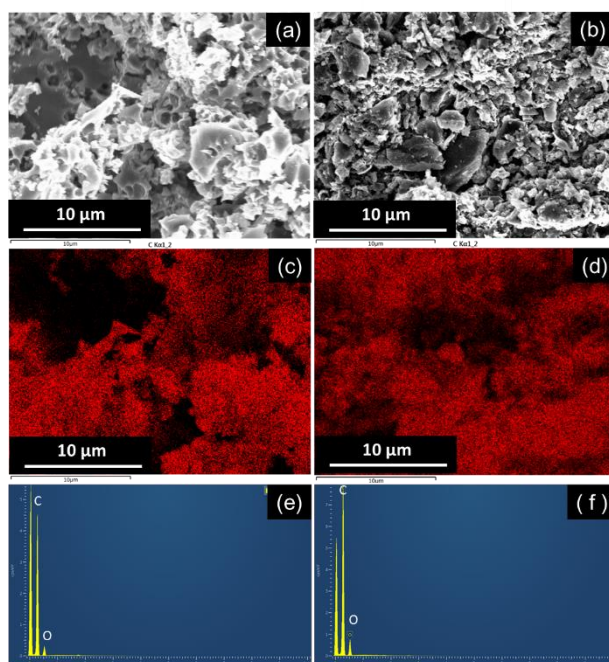


Figure 2. SEM images of AC_{Mn} (a) and AC_K (b) samples. Corresponding elemental mappings and spectra of AC_{Mn} (c, e) and AC_K (d, f) surface.

SEM and TEM was utilized to observe the morphologies and microstructures of the samples. The representative SEM images of the AC_{Mn} and AC_K are shown in Fig. 1(a) and Fig.1(b). From the images it is obvious that the structure of original bamboo is retained. Moreover, it is observed that plenty of pore macroporous structures with the pore diameter on the few macro were formed during the carbonization processes. These pores can not only facilitate the electrolyte penetration but also provide more electrochemically active sites.

According to the TEM images of the AC_{Mn} powder shown in Fig. 1(d) and (e), a rough edge and typical porous amorphous structure can be observed. In these TEM images, light regions correspond to pores and black regions correspond to carbon. The TEM images show that the sample is rich with a highly microporous structure. Well-developed small multi-pores, which are less than 200 nm, can also be observed. This continuous porous structure and hierarchical nano-architecture of the AC_{Mn} powder are favorable to improve the ion diffusion in supercapacitor.

However, more well-developed small multi-pores, which are less than 200 nm, can also be observed in the as-prepared AC_{Mn} powder (Fig. 1(c)). This continuous porous structure and hierarchical nano-architecture of the AC_{Mn} powder are favorable to improve the ion diffusion in supercapacitor.

Comparing with the macroporous structures of the AC_K sample observed from TEM image (Fig. 1(e)) and SEM image (Fig. 1(b)), the pore size is almost the same.

EDX analysis is a chemical analysis used in conjunction with SEM. The particular area was selected and the results obtained were shown in Fig.2. Almost only carbon and oxygen were detected in the samples. EDX peaks reveal that the AC_{Mn} and AC_K contains 89 wt% and 90 wt% of carbon, 10 wt% and 9 wt% of oxygen, respectively.

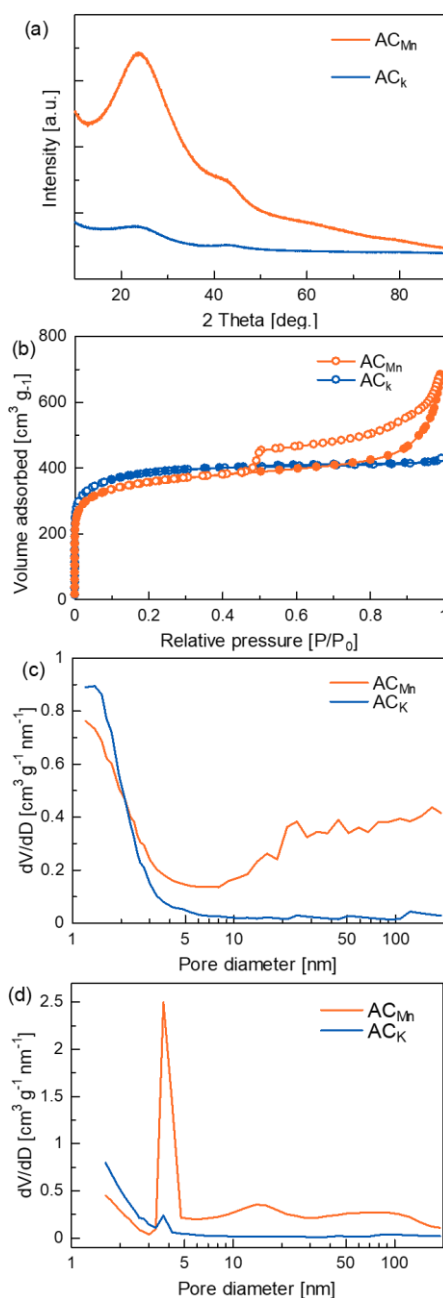


Figure 3. XRD patterns (a), N₂ adsorption–desorption isotherm (b), pore size distribution from the adsorption isotherm (c) and pore size distribution from the desorption isotherm (d) of the AC_{Mn} and AC_K samples.

XRD was used to characterize the graphitization degree of the samples. In Fig. 3(a), the diffraction pattern for the sample has two broad peaks at 26.5 and 44.4, which confirms the amorphous carbon structure of the sample.

The nitrogen adsorption-desorption measurement at 77K was carried out to evaluate porosity. The results are shown in Fig. 3(b). The isotherms of the two samples at low relative pressure exhibited similarity sharp adsorption inflection. It indicates that the samples have similar micropores and the pore size is smaller than 1 nm (Fig. 3(c)). Also, the AC_{Mn} sample has a lot of meso/macro porous textures, and the pore volume increases slowly with the pore diameter larger than 10 nm. This result is consistent with the observation of the TEM image (Fig. 1(c)). The pore size distribution curves from the desorption isotherm are showed in Fig.3(d). It is shown that AC_{Mn} sample has plenty of mesopore in the size about 3.7 nm with high pore volume. The values of BET specific surface area and the total pore volume are $915 \text{ m}^2/\text{g}$ and $930 \text{ m}^2/\text{g}$, and $1.05 \text{ cm}^3/\text{g}$ and $0.66 \text{ cm}^3/\text{g}$ for AC_{Mn} and AC_K , respectively. And it can be seen that the two samples possess different behavior at higher relative pressures. The result shows that the AC_{Mn} has mesoporous and macroporous textures. These results indicate that the volume of the mesoporous and macroporous increase by $KMnO_4$ activation process. It is expected that the $KMnO_4$ was used as both the activating agent K and Mn to fulfil the carbonization of bamboo carbon. And the Mn shows different effect from K to obtain meso-macroporus.

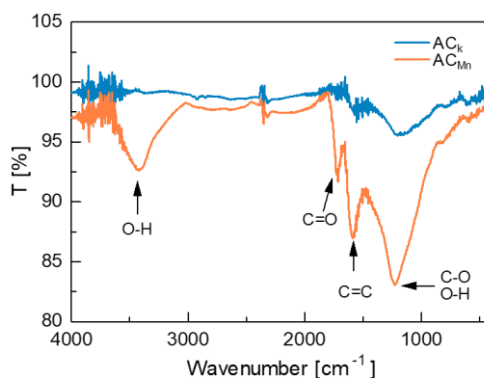


Figure 4. FTIR spectra of AC_{Mn} and AC_K samples.

Fig.4 shows the FTIR spectra for AC_{Mn} and AC_K samples in the mid-infrared region between 400 and 4000 cm^{-1} . The FTIR spectra for the AC_{Mn} sample has a wide band at 3400 cm^{-1} , which is ascribed to the O-H stretching vibration of hydroxyl and carboxyl. In addition, it exhibits two additional bands at 1600 cm^{-1} and 1720 cm^{-1} , which were attributed to the stretching vibration of the carboxyl groups of the C=C and C=O bonds, respectively. Furthermore, a significant difference was found in the range of 1000 to 1450 cm^{-1} , which was caused by the C-O (hydroxyl, ester, or ether) stretching vibration and the O-H bending vibration. Having stated the above, the activation processes of $KMnO_4$ and KOH have remarkable influence in the surface properties of the activated carbon materials. The AC_{Mn} has more functional groups of C=O and C=O. As a strong oxidizing agent, $KMnO_4$ improved the formation of oxygen-containing functional groups on the surface of the AC_{Mn} sample. These functional groups can

enhance the electrical conductivity and wettability of the activated carbon sample, thus guarantee the high performance of the electrode [18].

3.2 Electrochemical performance of electrodes

The electrochemical performance of AC_{Mn} and AC_K based electrodes was investigated using a three-electrode system. The CV measurements were conducted and the results are shown in Fig. 5(a). The CV profiles of the AC_{Mn} and AC_K based electrodes were evaluated at different potential scan rates (from 2 to 100 $mV s^{-1}$) which are controlled between $-0.2 V$ and $0.8 V$ versus the $Ag/AgCl$ reference electrode. As shown in Fig.5(a), the CV curves of the AC_{Mn} based electrode show a well symmetric rectangular shape with weakly broadened humps. This result indicates the obvious behavior of electrochemical double layer capacitance. The AC_K based electrode shows the same behavior as the AC_{Mn} electrode. The corresponding specific capacitance of the electrodes at various scan rates is also plotted in Fig. 3(b). The AC_{Mn} based electrode displays specific capacitance values of 225, 185, 164, 112, 74, and 30 F/g at the potential scan rates of 2, 5, 10, 30, 50, and 100 mV/s respectively. Moreover, the specific capacitance values of the based AC_K electrode are 209, 168, 112, 52, 31, and 15 F/g at the potential scan rates of 2, 5, 10, 30, 50, and 100 mV/s . The specific capacitance was similar with other study with different activating agent like KOH , K_2FeO_4 , $ZnCl_2$ [19-21]. With the increase of potential scan rate, the capacitance of the electrodes tends to decrease.

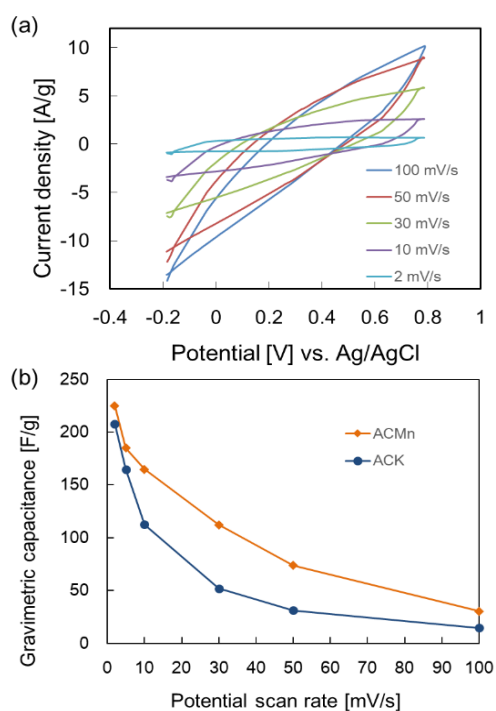


Figure 5. CV curves of AC_{Mn} based electrode at different potential scan rates (a); Specific capacitances of the AC_{Mn} and AC_K based electrode at various potential scan rates (b)

Table 1. Electrochemical performance of biomass-based activated carbon electrode.

Precursor	Activator	S _{BET} (m ² /g)	C _s (F/g)	Electrolyte	Ref
Bamboo	KMnO ₄	915	225	1 M H ₂ SO ₄	This work
Bamboo	KOH	930	209	1 M H ₂ SO ₄	This work
Bamboo stem	KOH	155	169	1 M H ₂ SO ₄	[22]
Bamboo solid residue	KOH	2150	160	1 M H ₂ SO ₄	[23]
Bamboo leaf	-	325	162	3 M KOH	[24]
Willow	-	739	93	6 M KOH	[25]
Ceder sawdust	KOH	1185	244	1M Na ₂ SO ₄	[26]

Table 1 shows the electrochemical performance of different biomass-based activated carbon electrode materials. The bamboo-based activated carbon electrodes exhibit a high specific capacitance of 225 F/g (AC_{Mn}) and 209 F/g (AC_K) at the potential scan rates of 2 mV/s, respectively, which are outperforming most existing data in the literature.

Although the rate capability is not impressive, compared with decreasing tendency of AC_K, the decrease rate of AC_{Mn} based electrode is clearly slower. According to the results, the remarkable electrochemical performance of the activated carbon sample synthesized using bamboo by KMnO₄ activation probable owing to the following aspects. Firstly, the micro-, meso-, and macro-structures can promote the penetration of electrolytic ions, which leads to good rate capability. Secondly, a great variety of surface functional groups can enhance the electrical conductivity and wettability of the activated carbon sample, thus guarantee the high performance of the electrode [27]. This work focus on finding a new chemical activating agent and manufacturing process with high performance micro-, meso-, and macro-structure. Based on this consideration, in this work the cyclic voltammetry techniques are used to confirm the basic electrochemical performance. As the future work, after confirming the performance of the structure further evaluations concerning the electrochemical performance are necessary.

4. CONCLUSIONS

In summary, activated carbon with unique micro-, meso-, and macro-structures has been successfully synthesized using bamboo powder by KMnO₄ activation and pyrolysis carbonization through a one-step strategy. The carbon possesses a porous structure with acceptable specific surface area of 915 m²/g and sufficient micropores. The electrode based on the carbon shows high specific capacitance (225 F/g at the potential scan rates of 2 mV/s). With the increase of potential scan rate, the specific capacitance of based AC_{Mn} based electrode tends to decrease. Compared with AC_k (activated by KOH) based electrode, the decreasing tendency of AC_{Mn}-based electrode is clearly slower. The results show that the KMnO₄ activation process of the bamboo powder can help to generate the meso-macro structure and more surface functional groups. These improved both storage capacity and transport behavior, and enhance the electrical conductivity and wettability of the activated carbon sample, thus guarantee the high performance of the electrode. As a result, the proposed one-step strategy using bamboo powder and KMnO₄ activation process has high potential to be develop highly efficient, green, low-cost and industrial-grade production of biomass-based activated carbon materials for many kinds emerging next generation environmental applications.

ACKNOWLEDGEMENTS

We gratefully acknowledge the financial support from the IWATANI NAOJI Foundation (18-4530). This work is also supported by JSPS KAKENHI Grant Number JP20K05108.

References

1. L. L. Zhang, and X.S. Zhao, *Chem. Soc. Rev.*, 38 (2009) 2520.
2. P. Simon, and Y. Gogotsi, *Acc. Chem. Res.*, 46 (2013) 1094.
3. A. Ghosh, and Y. Lee, *ChemSusChem*, 5 (2012) 480.
4. H. Chen, S. Zhou, and L. Wu, *ACS Appl. Mater. Interfaces*, 6 (2014) 8621.
5. Z. Li, D. Xiao, C. Xu, Z. Li, S. Bi, H. Xu, H. Dou and X. Zhang, *J. Mater. Sci.*, 57 (2022) 8818.
6. S. Yuan, W. Fan, Y. Jin, D. Wang and T. Liu, *Nano Mater. Sci.*, 3 (2021) 68.
7. Y. Li, Z. Li, B. Xing, H. Li, Z. Ma, W. Zhang, P. Reubroycharoen and S. Wang, *J. Anal. Appl. Pyrolysis*, 155 (2021) 105072.
8. M. Jayachandran, S. Kishore Babu, T. Maiyalagan, N. Rajadurai and T. Vijayakumar, *Mater. Lett.*, 301 (2021) 130335.
9. R. Farma, A. Putri, E. Taer, A. Awitdrus and A. Apriwandi, *J. Mater. Sci.: Mater. Electron.* 32 (2021) 7681.
10. J. Jiang, L. Zhang, X. Wang, N. Holm, K. Rajagopalan, F. Chen, and S. Ma, *Electrochim. Acta*, 113 (2013) 481.
11. C. S. Yang, Y.S. Jang, and H.K. Jeong, *Curr. Curr. Appl. Phys.*, 14 (2014) 1616.
12. Y. N. Gong, D. L. Li, C. Z. Luo, Q. Fu, and C. X. Pan, *Green Chem.*, 19 (2017) 4132.
13. S. Rezma1, I. B. Assaker, Y. litaiem, R. Chtourou, A. Hafiane1, H. Deleuze, *Mater. Res. Bull.*, 111 (2018) 222.
14. E. Taer, M. Sihombing, R. Taslim, Agustino and Apriwandi, *J. Phys. Conf. Ser.*, 5 (2020) 15.
15. J. Romanos, M. Beckner, T. Rash, L. Firlej, B. Kuchta, P. Yu, G. Suppes, C. Wexler and P. Pfeifer, *Nanotechnology*, 23 (2012) 015401.
16. M. Sevilla, C. Sanchís, T. Valdés-Solís, E. Morallón and A. B. Fuertes, *Carbon*, 46 (2008) 931.
17. Y. Wang, Y. Song, and Y. Xi, *Chem. Soc. Rev.*, 45 (2016) 5925.
18. S. Zhang and N. Pan, *Adv. Energy Mater.*, 5 (2015) 1401401.
19. K. M. Ajay, M.N. Dinesh, *Mater. Today: Proc.*, (2020).
20. Y. Gong, D. L. Li, C. Z. Luo, Q. Fu, and C. X. Pan, *Green Chem.*, 17 (2017) 132.
21. E. Taer, M. Sihombing, R. Taslim, Agustino and Apriwandi, *J. Phys. Conf. Ser.*, 1655 (2020) 012163.
22. E. Taer, L. Pratiwi, A. Apriwandi, W. S. Mustika, R. Taslim and A. Agustino, *Commun. Sci. Technol.*, 5 (2020) 22.
23. D. A. Khuong, H. N. Nguyen and T. Tsubota, *RSC Adv.*, 11 (2021) 9682.
24. Q. Wang, Y. Zhang, H. Jiang and C. Meng, *J. Colloid Interface Sci.*, 534 (2018) 142.
25. C. Jiang, G. A. Yakaboylu, T. Yumak, J. W. Zondlo, M. Edward and J. Wang, *Renew. Energy*, 155 (2020) 38.
26. L. Yang, Y. Feng, M. Cao and J. Yao, *Mater. Chem. Phys.*, 238 (2019) 121956.
27. D. Wang, Z. Geng, B. Li and C. Zhang, *Electrochim. Acta*, 173 (2015) 377.